RESEARCH ARTICLE

The spatial distribution of nests of the harvester ant *Messor barbarus* in dryland cereals

**J. M. Blanco-Moreno · P. R. Westerman ·
V. Atanackovic · J. Torra**

Abstract The harvester ant *Messor barbarus* can be responsible for substantial losses of weed seeds in arable fields in NE Spain. The spatial distribution of nests can have consequences for biological weed control, because foraging intensities decline with distance from the nest. The probability that seeds will escape harvesting will be lower if nests occur regularly distributed. We here investigated 'large'-scale variability (up to 150 m), caused by habitat heterogeneity, and 'small'-scale spatial variability (up to 12 m), caused by interactions between colonies, in nest distribution in a 50 × 150 m area in a cereal field in NE Spain, in 2009 and 2010. Large-scale variability was present in the data, but could not be explained by elevation, distance to the nearest field edge, or interpreted as simple trends across the area. Small-scale interactions could successfully be described by a multi-type/hard core Strauss process model, indicating territoriality among nests. Exclusion and inter-action zones were identified, with radii that were smaller for small than for large colonies, and smaller for 2009 than for 2010. There was close resemblance between the observed and fitted spatial structure up to a radius of 3–4 m. Large-scale spatial variability, but not small-scale interactions, may be responsible for the existence of areas with few or no nests, where weed seeds have a higher probability of escaping the ants and entering the seed bank. Identifying and understanding the factors that influence the large-scale trends is, therefore, essential for optimizing weed control.

Introduction

The harvester ant *Messor barbarus* (L.) is a common granivore in NE Spain. Inside rain-fed arable fields, it is by far the most abundant granivore and responsible for formidable losses of weed seeds. Depending on the weed species, 46–100 % of the newly produced weed seeds can be taken by the harvester ants (Westerman et al., 2012), thus contributing to weed control. Seed predation risk can vary considerably among and within fields (Baraibar et al., 2009, 2011). Differences in the spatial distribution of nests could be one of the factors responsible for the observed variability (Díaz, 1992; Azcárate and Peco, 2003; Baraibar et al., 2011). The probability that an arbitrary seed will escape being detected will be lower for a field in which nests are regularly distributed (underdispersed) than in a field in which nests occur in clumps (overdispersed). In the latter case, some areas may be searched more intensely than others, as foraging intensity declines exponentially with distance from the nest (Mull and Macmahon, 1997; Azcárate and Peco, 2003).

J. M. Blanco-Moreno (✉)
Departament de Biologia Vegetal, Facultat de Biologia,
Universitat de Barcelona, Av. Diagonal, 643, 08028 Barcelona,
Spain
e-mail: jmblanco@ub.edu

P. R. Westerman (✉)
Group Crop Health, Faculty of Agricultural and Environmental
Sciences, University of Rostock, Satower Str. 48, 18051 Rostock,
Germany
e-mail: paula.westerman@uni-rostock.de

V. Atanackovic · J. Torra
Department HBJ, University of Lleida, ETSEA, Av. Alcalde
Rovira Roure 191, 25198 Lleida, Spain

Ant colonies are territorial. For some species, it is known that they engage in nest-area marking by placing pheromones in the vicinity of a nest entrance to repulse alien workers (Grasso et al., 2005). Close to the nest, some species of ants are particularly aggressive to conspecifics from other colonies; aggression decreases with increasing distance from the nest entrance (Knaden and Wehner, 2003). Various factors, both biotic and abiotic, can influence nest distribution.

Differently aged colonies may display different spatial distribution patterns (Korb and Linsenmair, 2001). Once a year, mature colonies produce winged, reproductive males and females that are released after the first autumn rains. The locations where mated queens land are either randomly distributed or clumped (Ryti and Case, 1988; Grohmann et al., 2010), but the probability of successful nest initiation is strongly influenced by the proximity to long-established colonies (Ryti and Case, 1988; Grohmann et al., 2010). Workers of larger colonies harass and kill invading founding queens and destroy smaller, younger colonies (Baroni Urbani, 1968), while workers of younger colonies tend to be more tolerant (Grohmann et al., 2010). Estimates of the mortality rate of founding queens and first year colonies vary between 90 % (Ryti and Case, 1988) and >99 % (Gordon and Kulig, 1996). Survival probabilities of colonies remain low until they are about 2 years old (Johnson, 2001). Those colonies that have managed to survive the selective sieve of competition are expected to be spaced more regularly than young colonies.

A simulation study predicted more regular nest spacing with increasing nest density (Ryti and Case, 1988). At densities well below the carrying capacity, the distribution of young colonies in the non-occupied space will reflect the distribution of original landing sites of the foundresses. At densities close to the carrying capacity, the distribution of young nests will be shaped by competition with older nests. Variable resource density between years, and thus a variable carrying capacity, is expected to induce variability in establishment opportunities and intensity of intraspecific competition. Interestingly, these simulations showed that competition between older, established colonies was less likely to result in a regular distribution of nests (Ryti and Case, 1988).

For most ant species, for which the spatial distribution of nests was investigated, the distribution depended on the scale of observation. It is frequently regular or random at a fine spatial scale, but clumped at larger spatial scales (Schooley and Wiens, 2003; Folgarait et al., 2007). This phenomenon can partly be explained by large-scale biotic and abiotic factors that influence the survival chances of founding queens and young colonies. These include soil properties (Enzmann and Nonacs,

2010), topography (Kilpeläinen et al., 2008), amount and type of vegetation (Díaz, 1991), land use, level of disturbance, and field management (Díaz, 1991; Serrano et al., 1993; Folgarait et al., 2007; Baraibar et al., 2009). For example, soil strength, texture and moisture content of the top soil determine the ease with which ants can tunnel the soil and construct chambers (Boulton et al., 2005; Enzmann and Nonacs, 2010). Altitude, slope and orientation influence the number of hours that the ant nest is exposed to sunshine, which, in turn, influences ant activity and brood development (Crist and Williams, 1999; Wang et al., 2001; Azcárate et al., 2007).

Summarizing 160 studies involving 136 ant species, Levings and Traniello (1981) concluded that in the majority of the cases, nests were either regularly distributed (58), or randomly tending towards regularity (76). However, nests were also found to be randomly distributed (12 cases), randomly tending to clumped (4 cases), clumped (2 cases), or distributed as were the host plants (8 cases).

We were interested in the spatial distribution of nests of *M. barbarus* within arable fields, because of its potential consequences for biological weed control. The main purpose of this study was to provide a description of the spatial patterns of harvester ant nests. We quantified 'large'-scale variability (up to 150 m), caused by habitat heterogeneity, and 'small'-scale spatial variability (up to 12 m) in nest distribution, caused by interactions between colonies. We explored nest density and nest size as possible explanatory variables for small-scale spatial variability. Gibbs models with large-scale spatial trends were tested and evaluated, and the *L*-function was used to quantify the spatial structure of uni- and bivariate spatial patterns.

Materials and methods

Location

The spatial distribution of *M. barbarus* nests was determined in a no-till cereal field in Villanova de Bellpuig (41°35′25.76″N, 0°58′36.28″E) in NE Spain, shortly after crop harvest in July and August 2009 and 2010. For information on crop and soil management, we refer to the description of field 1B in Baraibar et al. (2009). In 2009, a 150 × 50 m area, at least 20 m from any field margin, was staked out, and its corners and perimeter were georeferenced, using a GPS with sub-metric precision (Trimble® GeoXHTM hand-held, GeoExplorer®, 2005). The area was retraced and reused in 2010. The area was subdivided into three 50 × 50 m blocks, and marked with sticks every 10 m for visual orientation and facilitation of nest counting.

Nest counts

Ant nests were identified by their conspicuous entrances. Because nests can have multiple entrances, the behaviour of the ants from nearby entrances was observed. When ants displayed aggression, avoidance or formed non-overlapping trails these were interpreted as signs that they belonged to different colonies. Only nests with visual ant activity were included in this study to avoid the inclusion of abandoned nests. Nests were labelled with coloured stakes to prevent double counting. Nests were counted and georeferenced (x, y coordinate, elevation) on 14 July, 22 July and 4 August in 2009, and on 10 August, 16 August, and 17 August in 2010, between 7 (sunrise) and 12 a.m., after which temperatures became prohibitive for ant activity (Azcárate et al., 2007). The shortest distance to the field edge was derived by GIS routines from a digital ortho-photomap at a scale of 1:5,000. The size of the nests was scored visually on a subjective scale from size 1 (smallest) to size 5 (largest). The scale was based on a combination of surface area occupied by the colony, number of entrances into the colony, and ant size and behaviour (Baraibar et al., 2011). A class 1 nest occupies ca. 0.40 m², has a single entrance, and no soldiers; class 2 nest, ca. 1 m², 1–2 entrances and no soldiers; class 3 nest, ca. 2 m², 2–3 entrances and soldiers; class 4 nest, 2–4 m², 3–4 entrances and soldiers; class 5 nests, >4 m², ≥5 entrances, soldiers and forms long, permanent columns. Only 32 nests fell into size class 4 and four into size class 5, which was considered insufficient to be analysed statistically. Therefore, nests were regrouped into category S_1 (size classes 1 and 2) and class S_2 (size classes 3, 4 and 5), which conveniently coincided with the distinction between those colonies that had a single nest entrance (S_1) and those that had multiple entrances and soldiers (S_2). It was implicitly assumed that nest size was related to colony age. But even if nest size was not directly related to colony age, no harm is done; size may be more important than age with respect to resource use and spatial distribution of nests (Kirkpatrick, 1984; Sauer and Slade, 1987), so results can be interpreted in terms of colony size (Gordon and Kulig, 1996).

Spatial point pattern analysis

The spatial distribution of *M. barbarus* nests can involve large-scale trends and small-scale variability. Large-scale trends are caused by habitat heterogeneity and small-scale variability by interactions between colonies. If large-scale trends are absent, a homogeneous Poisson process is the appropriate null model and the intensity function, λ, the expected number of nests per unit area, is constant. If large-scale trends are present, a heterogeneous Poisson process serves as a better null model, and λ is variable across space. After the trend is partialled out, the remaining deviations

from randomness are analysed to identify small-scale interactions between colonies. Interactions can involve a zone in which the probability of establishment of other colonies is increased (aggregated, clustered, overdispersed) or decreased (regular, underdispersed) and/or a zone from which other colonies are totally excluded.

Initially, the intensity function was related to elevation, distance to the nearest edge, and coordinates, covariates that may describe large-scale trends. However, since all attempts to establish such a relationship failed (data not shown), a non-parametric intensity function was adopted instead (Wiegand and Moloney, 2004), and no further mention was made of the covariates. The degree of smoothing involved in density estimation is a controversial issue (Wiegand and Moloney, 2004). Here, we opted for an intermediate degree of smoothing, namely a non-parametric estimate based on the Gaussian kernel with a bandwidth, h, of 10 m (Lan et al., 2012), which should preserve enough detail of the original data without being influenced by the distribution of individual nests.

The fit of several Gibbs models (Baddeley and Turner, 2006) was assessed, for each dataset (S_{11}, S_{22}, S_{12} and S_{21}) and each year (2009 and 2010), separately. Here, the variable S_{ij} refers to the interaction caused by colonies of size j around a colony of size i. Interactions occurring between nests of the same category caused univariate patterns, denoted as S_{11} and S_{22}, while interactions between nests belonging to two different nest size categories caused bivariate patterns, denoted as S_{12} and S_{21}. Within the class of heterogeneous Poisson process models, the basic heterogeneous Poisson model, the global Strauss model (GS), the multi-type Strauss (MS) and the multi-type/hard core Strauss models (MHS) were tested. The models differed in the way that they take nest size and type of interaction into account. The global Strauss model captures inter-nest repulsive interactions, but does not distinguish between categorical variables, such as nest size. It yields an interaction radius (ir), within which the probability of finding further nests is reduced, and an interaction strength, γ, for the pooled nest categories. An interaction parameter of zero indicates complete repulsion within the interaction radius; increasing values of γ indicate increasingly weaker interactions. The multi-type Strauss model allows for interaction radii and strengths of interactions for each nest category separately. The multi-type/hard core Strauss model distinguishes between a hard core radius (hr), a total exclusion zone around a nest, and an interaction zone (ir). The significance of each of the models was tested by means of 249 Monte Carlo simulations of the null model and refitting the null and the alternative models. Including the original fit, this yielded $n = 250$, which has a power efficiency of 0.4 %. Model fit was expressed as log-pseudo-likelihoods [log ($pLik$)]. The test statistic used was twice the log-pseudo-likelihood difference between the null and the

alternative models, analogous to the deviance, following Baddeley and Turner (2006). The heterogeneous Poisson model served as the null model. Profiled pseudo-likelihood was used to estimate ir, while hr was set to its maximum likelihood value (Baddeley and Turner, 2006).

A border correction of 5 m was applied to all estimation and model testing for practical reasons. This avoids computing the estimators of spatial structure with nests having fewer neighbours than expected, simply because they are close to the plot edges. The border correction width was set to a value larger than the estimated interaction radii of all models to be fitted (Baddeley and Turner, 2006).

For the best fitting model, the L-function was used as a summary statistic to quantify small-scale spatial structure, for each dataset (S_{11}, S_{22}, S_{12} and S_{21}). The L-function is a transformation of Ripley's K-function with $L(r) = \sqrt{K(r)/\pi}$. For the univariate pattern S_{11}, Ripley's $K(r) = \lambda^{-1}S_{11}$, with $K(r)$ the number of extra nests of category S_1 within distance r of a randomly chosen nest of category S_1, and λ the intensity function (Ripley, 1977). In the case of a homogeneous Poisson process, the expected value of $L(r)$ equals the radius r, and therefore $L(r)$–r has an expected value of zero. In the case of a heterogeneous Poisson process, $L(r)$–r is not zero, because of the presence of a large-scale trend, but the expected value and confidence interval can be calculated using Monte Carlo simulations. If the observed function lies outside the specified envelope, the tested model is rejected. Here, the expected values and the 95 % simultaneous critical envelopes were calculated using 249 simulations each.

All analyses were performed in R (version 2.12.1; R Development Core Team, 2010), using the package spatstat (Baddeley and Turner, 2006).

Results

Nest counts

In both years, nest densities were about 'normal' for the area ($\overline{x} = 468$ nests ha^{-1}; Baraibar et al., 2011). Overall, nest densities decreased from 2009 to 2010. In 2009, nest counts differed significant between blocks (Fisher's exact test, $p = 0.012$); block 2 harboured the lowest number of nests (71) and block 3 the highest (225) (Table 1). In 2010, blocks harboured similar total numbers of nests. From 2009 to 2010, the number of nests remained more or less stable in block 1, increased in block 2 and decreased in block 3.

In both years, there were more nests of category S_1 than S_2 in all blocks (Table 1). There were on average ($\pm$SE) 445 ± 147.2 nests/ha of category S_1, and 105 ± 35.8 nests/ha of category S_2 in 2009, and 347 ± 17.5 nests/ha of category S_1, and 80 ± 12.9 nests/ha of category S_2 in 2010.

Table 1 Number of *Messor barbarus* nests of size categories S_1 and S_2 in 2009 and 2010 in three 50×50 m blocks in a cereal field in NE Spain

Nest size	2009		2010	
	S_1	S_2	S_1	S_2
Block				
1	97	20	78	26
2	56	15	90	19
3	181	44	92	15

This means that on average, 21.4 ± 6.98 m^2 was available per colony in 2009 and 24.0 ± 0.32 m^2 in 2010. The difference in nest density between the two years could mainly be attributed to a 49 and 66 % reduction in block 3 in the number of small and large nests, respectively (Table 1). In the other two blocks, the number of large nests increased, while the number of small nests either decreased slightly (20 %; block 1) or increased (61 %; block 2).

The location of nests varied considerably between the 2 years, indicating strong temporal dynamics (Fig. 1). For example, in 2009, two concentrations of small nests covered the left side of the test area and another concentration was found in the top right corner (Fig. 1). In 2010, one of the concentrations on the right side had largely vanished and a new concentration of nests had appeared at the bottom middle of the area (Fig. 1). The location of large nests was equally dynamic.

Small-scale interactions

The fit of different classes of Gibbs models of inter-point interactions is summarized in Table 2. The log ($pLik$) was substantially enhanced in the models that assumed a heterogeneous Poisson process compared to the model that assumed a homogeneous Poisson process, and, therefore, large-scale spatial trends in nest density were present. When moving from simple to more complex models within the heterogeneous Poisson process models, increments in log ($pLik$) were relatively small. Nevertheless, in 2009, the fits of the GS model [Δlog ($pLik$) = 13], MS model [Δlog ($pLik$) = 17] and MHS model [Δlog ($pLik$) = 31] were better than that of the heterogeneous Poisson process and significant in all cases ($p \leq 0.004$). Similarly, in 2010, the fits of the GS model [Δlog ($pLik$) = 17], MS model [Δlog ($pLik$) = 21], and MHS model [Δlog ($pLik$) = 26] were better than that of the heterogeneous Poisson process and significant in all cases ($p \leq 0.004$).

For the MHS model, the hard core radius, i.e. the zone from which other colonies were totally excluded, ranged from 0.22 m (S_{11}) to 1.38 m (S_{22}) in 2009, and from 0.37 m (S_{11}) to 1.53 m (S_{22}) in 2010 (Table 3). In 2009, colonies
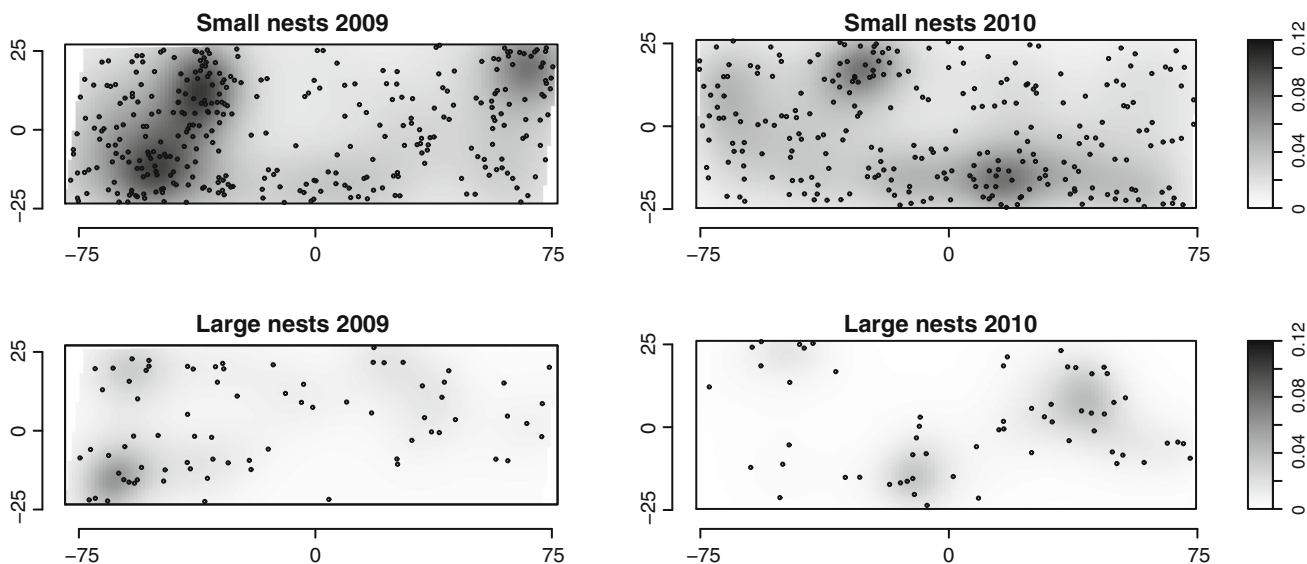
Fig. 1 Location of S_1 (*top*) and S_2 nests (*bottom*) of the harvester ants *Messor barbarus* in a 50 m by 150 m area in an arable field in NE Spain in 2009 (*left*) and 2010 (*right*). The *grey shading* represents nest densities (m^{-2} = 10^{-4} ha^{-1}) based on the kernel density estimate of the trend used in the inhomogeneous Poisson model

Table 2 Model fit for different Gibbs point process models, expressed as log-pseudo-likelihoods [log (*pLik*)], for data gathered in 2009 and 2010

Spatial model	2009	2010
Homogeneous Poisson	−1,783	−1,482
Heterogeneous Poisson	−1,244	−1,017
Global Strauss	−1,231	−1,000
Multi-type Strauss	−1,227	−995
Multi-type/hard core Strauss	−1,213	−991

Table 3 Estimated interaction radii, ir, interaction parameters, $\hat{\gamma}$, and hard core radii, hr, for interactions S_{11}, S_{12}, S_{22} and S_{21} based on the multi-type/hard core Strauss model

Interaction	2009			2010		
	hr (m)	ir (m)	γ	hr (m)	ir (m)	γ
S_{11}	0.22	0.85	0.45	0.37	1.12	0.29
$S_{12} = S_{21}$	0.54	1.63	0.43	0.93	1.38	1.40[a]
S_{22}	1.38	2.02	2.13[a]	1.53	2.81	0.76

[a] Estimate higher than its theoretical upper bound

influenced each other up to distances ranging from 0.85 m (S_{11}) to 2.02 m (S_{22}). Here, repulsion was moderately strong to weak (0.43 $\leq \hat{\gamma} \leq$ 2.13). In 2010, colonies interacted up to distances ranging from 1.12 m (S_{11}) to 2.81 m (S_{22}), and the interaction strength was stronger than in 2009 (0.29 $\leq \hat{\gamma} \leq$ 1.40). The estimates for γ_{22} in 2009 and γ_{12} in 2010 were higher than their theoretical upper bound, indicating that here the models were ill defined. Apparently, there was some aggregation at short distances of S_2 around

S_2 in 2009 and S_2 around S_1 in 2010 that the trend was not able to account for.

Summary statistic for small-scale interactions

In the case of the homogeneous Poisson model, the observed *L*-functions for S_{11} in 2009 and for S_{11} and S_{12} in 2010 lay partially outside the 95 % simultaneous critical envelopes, indicating that this model had to be rejected (data not shown). In addition, the functions for S_{12} in 2009 and S_{22} in 2010 were close to the confidence limits (data not shown).

Visual inspection of the *L*-functions for the MHS model (Fig. 2) indicated that explained short-range interactions fitted significantly better than did homogeneous Poisson or simpler heterogeneous models. Nowhere did the observed function, associated with the MHS model, cross the 95 % simultaneous critical envelopes. Up to a distance of 3–4 m, the observed functions (black lines) followed the expected functions (red lines) almost exactly, except in the case of S_{11} in 2010. This indicates that the short-range spatial structure was dominated by interactions between nests.

However, between 3–4 m and 12 m, the two functions diverged considerably. There are two possible explanations for this divergence. First, the non-parametric kernel did not adequately describe the large-scale trend and some other variable(s), not included in this study, was (were) responsible for the large-scale trends. Second, nests occurred indeed under- or overdispersed, with univariate interactions, i.e. S_1 nests around other S_1 nests (S_{11}) and S_2 nests around other S_2 nests (S_{22}) being regularly distributed (observed below expected function), and bivariate interactions (S_{12}
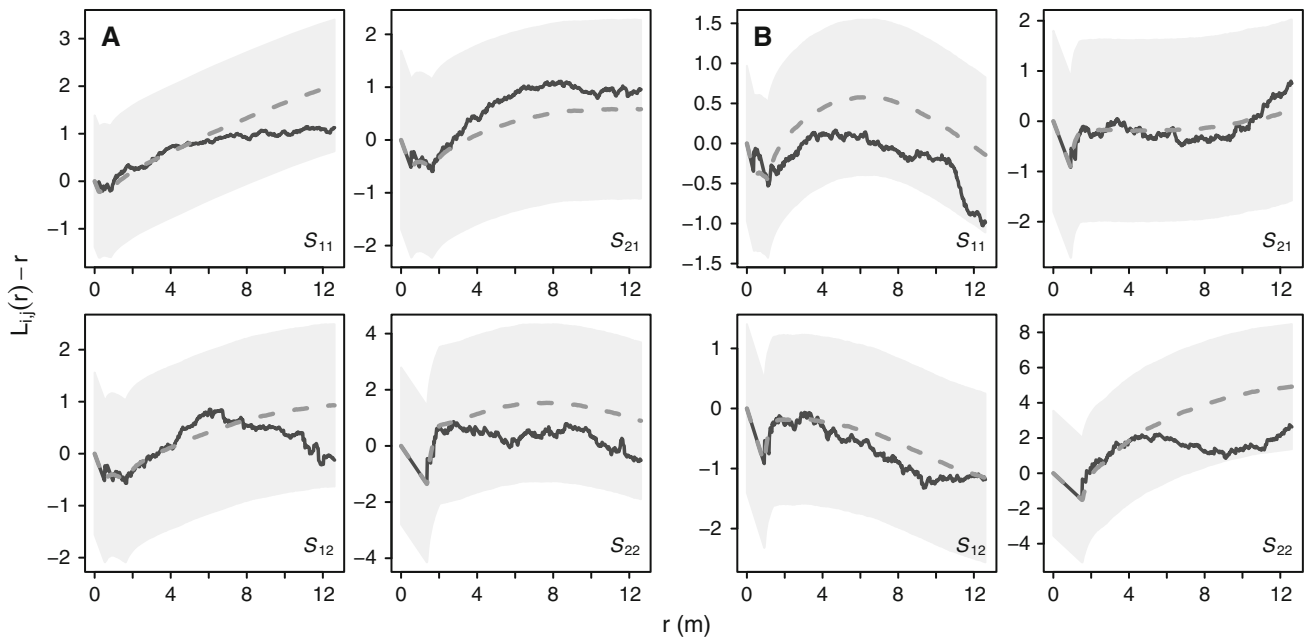
Fig. 2 Estimated $L(r)$–r as a function of r for each pair of nest categories, S_{11}, S_{12}, S_{22} and S_{21}, in 2009 (**a**) and 2010 (**b**), based on the multi-type/hard core Strauss model. The *dashed line* represents the expected value of the L-function under the heterogeneous Poisson process, while the *grey band* represents the simultaneous 95 % critical envelopes

and S_{21}) either overdispersed (expected below observed) or variable with increasing radii.

Discussion

At a fine spatial scale (≤ 4 m), *M. barbarus* nests were regularly distributed. We found evidence of exclusion zones, hr, the zone around a nest entrance from which other colonies were completely excluded, and interaction zones, ir, the zone within which the probability of finding further nests is reduced, indicating territoriality.

Territoriality differed between nest size categories. When measured by the radii of hr and ir, territoriality was stronger for large than for small nests. For example, the radii of hr were considerably larger for S_{22} (1.4–1.5 m) than for S_{11} (0.2–0.4 m). The exclusion zone could represent the surface area underneath which the actual, physical nest is located. The radii of the ir were also larger for S_{22} (1.5–2.8 m) than S_{11} (0.9–1.2 m). Interestingly, the radii of both hr and ir for dealings between small and large colonies (S_{12} and S_{21}) were intermediate between those for S_{11} or S_{22}, suggesting that large colonies were less territorial towards small colonies. When measured by the interaction strength within the interaction zone, γ, territoriality tended to be stronger for small than for large colonies. The interaction strength gives an indication of how strongly the territory is being defended by the resident nest. Consequently, although the size of the territory was smaller for small than for large

colonies, smaller territories seem to be defended more fiercely than large territories.

Territoriality also differed between years. For both S_{11} and S_{22}, the radii of hr and ir were larger in 2010 than 2009. Furthermore, the value of the interaction strength, γ, indicated that repulsion in the interaction zone tended to be stronger in 2010 than in 2009. This combination, larger radii and stronger repulsion, would be consistent with a situation in which resource availability was lower in 2010 than in 2009, forcing colonies to extend their territories and to defend these territories more strongly to meet their dietary needs. This situation could have arisen from increasing ant population density or from decreasing seed availability between 2009 and 2010. We do not have information on weed seed production, so cannot rule out the possibility that the resource availability differed between years. However, we do have (weak) indications that suggest that the ant population density may have been above its carrying capacity. Usually, nest densities in the area reach a peak about 11–12 years after the conversion from conventional to no-till soil management (Baraibar et al., 2011). After that, nest densities tend to decrease again, presumably because the ant density is above its carrying capacity, which is corrected through competition. In 2009, this particular field had not been tilled for 16 years, and it is possible that the ant population was in the process of eliminating surplus colonies. This would explain why the nest density was, on average, lower in 2010 than in 2009. This apparent contradiction, higher ant densities corresponding with lower

nest densities, originates from the fact that the number of ants per nest can increase. The above explanation could be verified in future research by focussing on ant densities, rather than nest densities. Furthermore, differences in the dynamics of nest densities between blocks suggest that ant population density and/or resource availability can vary considerably at a fine spatial scale.

Assuming that nest size was indicative of colony age, we found no evidence for the prediction that older colonies would be more regularly dispersed than younger colonies, at least not at a small scale. A difference in the radii of hr and ir between small and large nests is in itself no evidence that one or the other is more regularly dispersed; it simply tells how densely ant colonies can be packed spatially. Both categories of nests were regularly distributed, but the number of small nests per surface area could be higher than that of large nests. Furthermore, the weaker repulsion between large nests (higher γ for S_{22} than for S_{11}) indicates that the small-scale distribution of large nests could be less regular than that of small nests. In addition, it was predicted that the distribution of nests would be more regular at high than at low nest densities. *Messor barbarus* nest density was 22.5 % lower in 2010 than in 2009, and we, therefore, expected a more regular distribution of nests in 2009. Again, we found no evidence for this prediction, at a small spatial scale. In fact, interactions were almost always stronger (lower γ) in 2010 than in 2009, which is at odds with the initial prediction.

Large spatial trends (>12 m), not linearly related to x- or y-coordinates, were present in the distribution of *M. barbarus* nest across the 50×150 m area in both years. However, we were unsuccessful at relating large spatial trends to the chosen abiotic factors; distance to the field edge, altitude or field coordinates (see Materials and Methods). The choice of these factors was prompted mainly by practical reasons, e.g. easily measurable; nevertheless, the choice of factors was not farfetched, because all three factors separately had been successfully related to the distribution of harvester ants in other studies. The fact that the large-scale distribution in our data was so variable between the 2 years (Fig. 1) was unexpected, because it is known that ant colonies can persist at least 12 years, the average age of queens (X. Espadaler, pers. comm.). Furthermore, relocation of nests is rare in this species (P.R. Westerman, pers. obs.), similar to that in other species (Gordon, 1992), suggesting that the dynamics between the 2 years was largely caused by mortality of existing colonies and establishment of new colonies. This again suggests that the origin of the spatial trend should not be sought in static factors, i.e. most abiotic factors, such as altitude or soil type. Instead the origin of the spatial trend should be sought in some dynamic factor(s), i.e. most biotic factors. Examples of such dynamic, biotic factors are seed availability,

microclimate, soil surface conditions, strength of intraspecific competition or the distribution of landing sites of foundresses. Finding and understanding the origin of large-scale trends is important, because these were responsible for the observed peaks and troughs in nest density across space, not the small-scale interactions. This again is relevant for weed management, because, in areas void of nests, weed seeds will have a higher probability of escaping predation by *M. barbarus* and entering the seed bank.

The results of this study indicate that if weed seeds escape predation by the harvester ant, *M. barbarus*, this will be mainly due to large-scale trends and not due to small-scale interactions between colonies. At a small scale, nests were all more or less regularly distributed. Identifying and understanding the factors that influence the large-scale trends is, therefore, essential for optimizing biological weed control by harvester ants. We now know that the factors that influence the large-scale trend are likely to vary considerably from year to year, which means that our current choice of factors was inappropriate, because they were static. However, many other biotic and abiotic factors, not quantified here, could potentially be linked to the large-scale trend, which could then explain the observed patterns and help manage these beneficial insects.

References

Azcárate F.M., Kovacs E. and Peco B. 2007. Microclimatic conditions regulate surface activity in harvester ants *Messor barbarus*. *J. Insect Behav.* **20**: 315–329.

Azcárate F.M. and Peco B. 2003. Spatial patterns of seed predation by harvester ants (*Messor* Forel) in Mediterranean grassland and scrubland. *Insect. Soc.* **50**: 120–126.

Baddeley A. and Turner R. 2006. Modelling spatial point patterns in R. In: *Case Studies in Spatial Point Pattern Modelling, No. 185 in Lecture Notes in Statistics* (Baddeley A., Gregori P., Mateu J., Stoica R. and Stoyan D., Eds). Springer, New York, pp 23–74.

Baraibar B., Torra J. and Westerman P.R. 2011. Harvester ant (*Messor barbarus* (L.)) density as related to soil properties, topography and management in semi-arid cereals. *Appl. Soil Ecol.* **5**: 60–65.

Baraibar B., Westerman P.R., Carrión E. and Recasens J. 2009. Effects of tillage and irrigation in cereal fields on weed seed removal by seed predators. *J. Appl. Ecol.* **46**: 380–387.

Baroni Urbani C. 1968. Monogyny in ant societies. *Zool. Anz.* **181**: 269–277.

Boulton A.M., Davies K.F. and Ward P.S. 2005. Species richness, abundance, and composition of ground-dwelling ants in northern California grasslands: role of plants, soil, and grazing. *Environ. Entomol.* **34**: 96–104.

Crist T.O. and Williams J.A. 1999. Simulation of topographic and daily variation in colony activity of *Pogonomyrmex occidentalis* (Hymenoptera: Formicidae) using a soil temperature model. *Environ. Entomol.* **28**: 659–668.

Díaz M. 1991. Spatial patterns of granivorous ant nest abundance and nest site selection in agricultural landscapes of Central Spain. *Insect. Soc.* **38**: 351–363.

Díaz M. 1992. Spatial and temporal patterns of granivorous ant seed predation in patchy cereal crop areas of central Spain. *Oecologia* **91**: 561–568.

Enzmann B.L. and Nonacs P. 2010. Digging beneath the surface: incipient nest characteristics across three species of harvester ant that differ in colony founding strategy. *Insect. Soc.* **57**: 115–123.

Folgarait P.J., Gorosito N., Pizzio R., Rossi J.P. and Fernández J. 2007. *Camponotus punctulatus* ant's demography: a temporal study across land-use types and spatial scales. *Insect. Soc.* **54**: 42–52.

Gordon D.M. 1992. Nest relocation in harvester ants. *Ann. Entomol. Soc. Am.* **85**: 44–47.

Gordon D.M. and Kulig A.W. 1996. Founding, foraging, and fighting: colony size and the spatial distribution of harvester ant nests. *Ecology* 77: 2393–2409.

Grasso D.A., Sledge M.F., Le Moli F., Mori A. and Turilazzi S. 2005. Nest-area marking with faeces: a chemical signature that allows colony-level recognition in seed harvesting ants (Hymenoptera, Formicidae). *Insect. Soc*. **52**: 36–44.

Grohmann C., Oldeland J., Stoyan D. and Linsenmair K.E. 2010. Multi-scale pattern analysis of a mound-building termite species. *Insect. Soc.* **57**: 477–486.

Johnson R.A. 2001. Biogeography and community structure of North American seed-harvester ants. *Annu. Rev. Entomol.* **46**: 1–29.

Kilpeläinen J., Punttila P., Finér L., Niemla P., Domisch T, Jurgensen M.F., Neuvonen S., Ohashi M., Risch A.C. and Sundström L. 2008. Distribution of ant species and mounds (*Formica*) in different-aged managed spruce stands in eastern Finland. *J. Appl. Entomol.* **132**: 315–325.

Kirkpatrick M. 1984. Demographic models based on size, not age, for organisms with indeterminate growth. *Ecology* **65**: 1874–1884.

Knaden M. and Wehner R. 2003. Nest defense and conspecific enemy recognition in the desert ant *Cataglyphis fortis*. *J. Insect Behav.* **16**: 717–730.

Korb J. and Linsenmair K.E. 2001. The causes of spatial patterning of mounds of a fungus-cultivating termite: results from nearest-neighbour analysis and ecological studies. *Oecologia* **127**: 324–333.

Lan G., Getzin S., Wiegand T., Hu Y., Xie G., Zhu H and Cao M. 2012. Spatial distribution and interspecific associations of tree species in a tropical seasonal rain forest of China. *PLOS ONE* 7: e46074.

Levings S.C. and Traniello J.F.A. 1981. Territoriality, nest dispersion, and community structure in ants. *Psyche* **88**: 265–319.

Mull J.F. and Macmahon J.A. 1997. Spatial variation in rates of seed removal by harvester ants (*Pogonomyrmex occidentalis*) in a shrub-steppe ecosystem. *Am. Midl. Nat.* **138**: 1–13.

R Development Core Team 2010. R: A language and environment for statistical computing. R foundation for statistical computing, Austria. www.R-project.org. Accessed 18 November 2013.

Ripley B.D. 1977. Modelling spatial patterns. *J. R. Stat. Soc. B* **39**: 172–212.

Ryti R.T. and Case T.J. 1988. The regeneration niche of desert ants: effects of established colonies. *Oecologia* **75**: 303–306.

Sauer J.R. and Slade N.A. 1987. Uinta ground squirrel demography: is body mass a better categorical variable than age? *Ecology* **68**: 642–650.

Schooley R.L. and Wiens J.A. 2003. Spatial patterns, density dependence, and demography in the harvester ant, *Pogonomyrmex rugosus,* in semi-arid grasslands. *J. Arid Environ*. **53**: 183–196.

Serrano J.M., Acosta F.J. and Lopez F. 1993. Belowground space occupation and partitioning in an ant community during succession. *Eur. J. Entomol.* **90**: 149–158.

Wang C., Strazanac J.S. and Butler L. 2001. Association between ants (Hymenoptera: Formicidae) and habitat characteristics in oak-dominated mixed forests. *Environ. Entomol.* **30**: 842–848.

Westerman P.R., Atanackovic V., Royo-Esnal A. and Torra J. 2012. Differential weed seed removal in dryland cereals. *Arthropod-Plant Interact.* **6**: 591–599.

Wiegand T. and Moloney K.A. 2004. Rings, circles, and null-models for point pattern analysis in ecology. *Oikos* **104**: 209–229.